Eur J Nucl Med Mol Imaging (2014) 41:343–349
DOI 10.1007/s00259-013-2607-4

ORIGINAL ARTICLE

High-resolution imaging of pulmonary ventilation and perfusion with ^{68}Ga-VQ respiratory gated (4-D) PET/CT

Jason Callahan · Michael S. Hofman · Shankar Siva · Tomas Kron · Michal E. Schneider · David Binns · Peter Eu · Rodney J. Hicks

Received: 12 August 2013 / Accepted: 4 October 2013 / Published online: 6 November 2013

Abstract
Purpose Our group has previously reported on the use of ^{68}Ga-ventilation/perfusion (VQ) PET/CT scanning for the diagnosis of pulmonary embolism. We describe here the acquisition methodology for ^{68}Ga-VQ respiratory gated (4-D) PET/CT and the effects of respiratory motion on image coregistration in VQ scanning.
Methods A prospective study was performed in 15 patients with non-small-cell lung cancer. 4-D PET and 4-D CT images were acquired using an infrared marker on the patient's abdomen as a surrogate for breathing motion following inhalation of Galligas and intravenous administration of ^{68}Ga-macroaggregated albumin. Images were reconstructed with phase-matched attenuation correction. The lungs were contoured on CT and PET VQ images during free-breathing (FB) and at maximum inspiration (Insp) and expiration (Exp). The similarity between PET and CT volumes was measured using the Dice coefficient (DC) comparing the following groups; (1) FB-PET/CT, (2) InspPET/InspCT, (3) ExpPET/Exp CT, and (4) FB-PET/AveCT. A repeated measures one-way ANOVA with multiple comparison Tukey tests were performed to evaluate any difference between the groups. Diaphragmatic motion in the superior–inferior direction on the 4-D CT scan was also measured.
Results 4-D VQ scanning was successful in all patients without additional acquisition time compared to the nongated technique. The highest volume overlap was between ExpPET and ExpCT and between FB-PET and AveCT with a DC of 0.82 and 0.80 for ventilation and perfusion, respectively. This was significantly better than the DC comparing the other groups (0.78–0.79, $p<0.05$). These values agreed with a visual inspection of the images with improved image

Jason Callahan and Michael S. Hofman contributed equally to this work.

Electronic supplementary material The online version of this article (doi:10.1007/s00259-013-2607-4) contains supplementary material, which is available to authorized users.

J. Callahan (✉)
Peter MacCallum Cancer Centre, Centre for Molecular Imaging, St Andrews Place, East Melbourne, VIC, Australia
e-mail: jason.callahan@petermac.org

M. S. Hofman
Department of Medicine, Peter MacCallum Cancer Centre, Centre for Molecular Imaging, The University of Melbourne, St Andrews Place, East Melbourne, VIC, Australia

S. Siva
Peter MacCallum Cancer Centre, Department of Radiation Oncology, The University of Melbourne, St Andrews Place, East Melbourne, VIC, Australia

S. Siva · T. Kron
Sir Peter MacCallum Department of Oncology, The University of Melbourne, St Andrews Place, East Melbourne, VIC, Australia

T. Kron
Peter MacCallum Cancer Centre, Department of Physical Sciences, The University of Melbourne, St Andrews Place, East Melbourne, VIC, Australia

M. E. Schneider
Department of Medical Imaging and Radiation Science, Monash University, Wellington Rd, Clayton, VIC, Australia

D. Binns · P. Eu
Peter MacCallum Cancer Centre, Centre for Cancer Imaging, St Andrews Place, East Melbourne, VIC, Australia

R. J. Hicks
Sir Peter MacCallum Department of Oncology, Peter MacCallum Cancer Centre, Centre for Molecular Imaging, The University of Melbourne, St Andrews Place, East Melbourne, VIC, Australia

coregistration around the lung bases. The diaphragmatic motion during the 4-D CT scan was highly variable with a range of 0.4–3.4 cm (SD 0.81 cm) in the right lung and 0–2.8 cm (SD 0.83 cm) in the left lung. Right-sided diaphragmatic nerve palsy was observed in 3 of 15 patients. *Conclusion* ^{68}Ga-VQ 4-D PET/CT is feasible and the blurring caused by respiratory motion is well corrected with 4-D acquisition, which principally reduces artefact at the lung bases. The images with the highest spatial overlap were the combined expiration phase or FB PET and average CT. With higher resolution than SPECT/CT, the PET/CT technique has a broad range of potential clinical applications including diagnostic algorithms for patients with suspected pulmonary embolism, preoperative evaluation of regional lung function and improving assessment or understanding of pulmonary physiology in the vast range of pulmonary diseases.

Keywords ^{68}Ga-ventilation/perfusion PET/CT · Respiratory gated PET/CT · Pulmonary embolism · Respiratory motion

Introduction

It has been 50 years since Henry N. Wagner's first description of pulmonary lung perfusion imaging using macroaggregated albumin (MAA) [1]. The technique remains in widespread use around the world, primarily for assessment of suspected pulmonary embolism. However, it also has applications in many other clinical settings including quantitative assessment of lung function. Advances over the last five decades have included SPECT, SPECT/CT hybrid imaging and the use of newer radiotracers for inhalation, particularly microparticulate aerosols such as Technegas (Cyclomedica, Lucas Heights, Australia) [2–4].

The availability of the ^{68}Ge/^{68}Ga generator in recent years has opened up a whole new era of exploration in molecular imaging. This is a radionuclide generator, similar to the ^{99}Mo/^{99m}Tc generator, that produces the positron-emitting isotope ^{68}Ga. ^{68}Ga is a versatile isotope that can be used to label a wide range of tracers previously the domain of gamma-emitting isotopes such as ^{99m}Tc and ^{111}In. The most successful and well-documented of these are the somatostatin analogues DOTA-TOC and DOTA-TATE [5, 6]. This ability to label established tracers with a ready source of a positron-emitting isotope has provided the opportunity to exploit the superior imaging characteristics of the PET camera over the gamma camera [7]. One new area of investigation is the use of ^{68}Ga-labelled carbon nanoparticles (Galligas) and MAA (^{68}Ga-MAA) to perform a ventilation/perfusion (VQ) scan on a PET scanner [8–10].

Our group has previously reported the potential advantages of VQ PET/CT in a pilot series of patients being investigated for pulmonary embolism [11]. In this series it was found that the image quality was either equivalent or superior to VQ SPECT/CT. In addition, it was found that in both free-breathing (FB) SPECT and PET there was misregistration between SPECT/CT and PET/CT scans due to the effects of respiratory motion. Respiratory motion reduces quality due to blurring of activity in addition to inaccurate attenuation correction due to CT misregistration. The newest generation of PET/CT scanners allow the acquisition of multiple bed-step respiratory-gated (4-D) PET and CT scans. This acquisition technique potentially provides imaging in both inspiration and expiration cycles.

In this work we investigated the effects of respiratory motion on VQ scanning. We describe the acquisition parameters, and assess which phases of respiratory gating produce images with the highest spatial overlap between PET and CT. It was our hypothesis that 4-D imaging would improve coregistration between PET and CT modalities enabling the ability to quantify regional lung function more accurately, which is of particular relevance to predicting outcomes of lung surgery or radiotherapy.

Materials and methods

Patients

Fifteen patients (ten men, five women) were prospectively recruited as part of a study assessing serial change in lung function during radiotherapy (Australian New Zealand Clinical Trial Registry Trial ID 12613000061730). All patients had locally advanced or inoperable non-small-cell lung cancer and radiation therapy with curative intent was planned in all patients. The mean age of the patients was 67 years (range 46 – 88 years). This patient cohort consisted largely of ex-smokers with preexisting airways disease, with a mean forced expiratory volume in 1 s (FEV1) of 1.87 l (0.83 – 2.82 l) and carbon monoxide diffusing capacity (DLCO) of 54 % (27 – 87 %). Exclusion criteria included major airways reversibility demonstrated on pulmonary function testing, defined as a change in FEV1 of greater than 200 ml and 15 % predicted after the introduction of a bronchodilator. All patients were to complete a ^{68}Ga-VQ 4-D PET/CT scan prior to commencement of radiation therapy. The study was approved by the Peter MacCallum Clinical Governance and Ethics Committee, and all patients provided written informed consent.

PET/CT protocol

A ^{68}Ga-VQ 4-D PET/CT scan was performed on all 15 patients. The scan consisted of three parts:

1. 4-D CT
2. 4-D ventilation PET
3. 4-D perfusion PET

The patient was positioned supine on a GE Discovery 690 PET/CT scanner (GE Medical Systems Milwaukee, WI) in a default planning position using the radiotherapy palette and head rest with arms raised. The extension tubing attached to the intravenous cannula was placed in an easily accessibly position to allow administration of the ^{68}Ga-MAA without requiring the patient to move between ventilation and perfusion scans. The patient's breathing was tracked using a Varian RPM respiratory tracking system (Varian Medical Systems, Palo Alto, CA). The patients were instructed to breathe freely for the duration of the scans. No breathing training or coaching was used.

Galligas inhalation

Galligas was prepared using a Technegas generator (Cyclopharm) as described previously [11]. Approximately 200 MBq of ^{68}Ga was added to the carbon crucible. The patients were placed in a supine position and inhaled Galligas using the standard ventilation technique. A Gammasonics 450P (Gammasonics Pty Ltd, Five Dock, NSW, Australia) Geiger counter was used to measure the amount of inhaled gas. The monitor was placed over each lung and the highest detected dose rate was recorded in microsieverts per hour. The dose rate over the lungs was recorded to determine the association between the Geiger counter and PET camera count rate.

4-D CT acquisition

A scout scan was performed to plan the scanned area. The axial extent of the 4-D CT scan was determined as the length of two PET bed positions. The top of the field of view was aligned with the apex of the lungs. The positions for the ventilation and perfusion CT scans were matched. After moving the patient into position, the breathing was allowed to stabilize and recorded using the Varian RPM system. The Varian RPM system uses an infrared camera to track the motion of a box placed on a the patient's abdomen. Once the breathing had stabilized a 4-D CT scan was performed using the following parameters: cine CT, 10 mA, 140 kV, cine duration = breathing period + 1.5 s, and the cine time between images = breathing period/10. These exposure parameters produced an average CT dose index (CTDI) of 5.9 mGy and dose–length product of 169 mGy-cm. After completion of the 4-D CT scan, the respiratory trace was saved and a new trace was established to use for the ventilation PET scan.

4-D-ventilation PET

The patient was moved into PET position and the breathing was allowed to stabilize again before beginning the ventilation PET scan. This was acquired over two bed positions as a list-mode acquisition while recording the patient's breathing trace. Each bed position was acquired for 5 min, but this could be increased at the operator's discretion if the count rate was low due to poor inhalation or due to a low administered dose of Galligas.

4-D perfusion PET

^{68}Ga-MAA was prepared using the process described in our previous paper [11]. A mean dose of 50 MBq (range 21 – 62 MBq) ^{68}Ga-MAA was dispensed into a Braun Injekt® 2-ml syringe to minimize residual activity. Without the patient moving, the ^{68}Ga-MAA was injected through the extension tube with repeated flushing of the syringe with 20 ml of normal saline. A new respiratory trace was then established and allowed to stabilize. Once the new trace had been started, the perfusion PET scan was the acquired for 5 min per bed step. The perfusion PET scan was also acquired as a two-bed, list-mode acquisition in the same position as the ventilation scan. The count rate for the perfusion scan was recorded for comparison with the ventilation count rate.

Image reconstruction

The 4-D CT data were reconstructed using the GE Advantage4-D processing package (v 1.01-1p). Using the Varian respiratory trace the data were retrospectively binned equally in the five bins based on a percentage of the respiratory cycle with the first phase representing the end-inspiration position and the third phase the end-expiration position. A 4-D CT average (AveCT) reconstruction was also produced for each scan. AveCT reconstruction is created by using the average radiodensity across the five respiratory bins.

The ventilation and perfusion PET data were reconstructed as FB static scans using the end-inspiration CT data for attenuation correction. The data were also retrospectively binned into five bins based on a percentage of the respiratory cycle using GE automatic phase matching. This automatically matches each PET bin to the respective CT bin for attenuation correction. The FB-PET and 4-D PET images were reconstructed using ordered subset expectation maximization iterative reconstruction using the following parameters: four iterations, nine subsets, 192 matrix, 5-mm Gaussian smoothing.

4-D image registration data analysis

The lungs were contoured using MIMimage analysis software (MIM 5.4.4; MIM Software, Cleveland, OH) on the following datasets:

1. CT: AveCT, InspCT, ExpCT
2. Ventilation: FB-Vent, InspVent, ExpVent
3. Perfusion: FB-Perf, InspPerf, ExpPerf

The lungs in all three CT datasets were contoured using an upper Hounsfield unit value of −150. Due to the significant heterogeneity caused by the prevalence of airways disease in

this patient population, there were no PET automatic contouring methods that could be applied to all patients. Therefore, a visually adapted threshold was applied to the PET data to contour the ventilation and perfusion scans using the region growing tool. A standardized uptake value threshold was determined on the FB-Vent and FB-Perf images by a single experienced observer. The contours were then confirmed by a nuclear medicine physician. The threshold selected was optimized to include all areas of tracer accumulation in the lung and any accumulation of tracer in the main bronchi was manually excluded. The same threshold was then applied to the inspiration and expiration datasets. Any normal structures such as trachea and stomach were manually excluded from the contoured volume.

The amount of diaphragmatic motion at the most cranial convexity of the diaphragm was also measured in the craniocaudal direction from the 4-D CT images. In the coronal plane the distance from end-inspiration to end-expiration was measured at the level of the carina. The spatial overlap between PET and CT contoured lung volumes was compared using the Dice coefficient (DC) [12]. The DC was calculated using the MIM image analysis software. A DC of 1 indicates perfect concordance between volumes, whereas a value of 0 indicates no concordance between volumes. The DC can be represented using the following formula:

$$DC = \frac{2(CTvol \cap PETvol)}{(CTvol + PETvol)}$$

The DC comparing PET and CT volumes were compared in the following groups: (1) FB-PET/CT (end-InspCT), (2) InspPET/InspCT, (3) ExpPET/ExpCT, and (4) FB-PET/AveCT for both the ventilation and perfusion PET studies.

Statistical analysis

All statistical tests were carried out using GraphPad Prism 5 (La Jolla, CA, USA). A repeated measures one-way ANOVA with multiple comparison post hoc Tukey test's was performed to determine the significance of any differences between the groups. A p-value of <0.05 was deemed significant. A linear regression analysis was performed to determine the correlation between ventilation dose rates on the Geiger counter and count rates on the PET camera.

Results

Ventilation scan count rate: Geiger counter vs. PET scanner

A linear regression analysis of the count rates measured on the Geiger counter in microsieverts per hour versus the count rates measured on the PET camera in kilocounts per second (KCPS) revealed an r^2 value of 0.67 (Fig. 1). The average dose rate achieved on the Geiger counter was 37 μSv/h, which equated to an average count rate on the camera of 31 KCPS. Due to shortage of ^{68}Ga from an ageing generator and poor patient compliance, the ventilation count rate in 2 of 15 patients was only 10 KCPS. While the FB-PET was diagnostic in these patients, the count rate for the 4-D-ventiation scan was too low for analysis, and these studies were excluded from the analysis.

Ventilation vs. perfusion count rates

The mean count rate for the perfusion scans was 203 KCPS. The count rate was on average 7.8 times greater on the perfusion scans than on the ventilation scans. However, in one patient there was significant trapping of the Galligas in the central airways and insufficient ^{68}Ga-MAA was injected due to production problems. This led to a suboptimal VQ ratio (3.2 times) producing shine-through of the Galligas into the perfusion scan. However, despite residual counts from the preceding ventilation study contributing to apparent activity on the perfusion scan, the study was still considered of sufficient quality to be included in the analysis.

Lung motion

The diaphragmatic motion during the 4-D CT scans was highly variable with a range of 0.4 – 3.4 cm (SD 0.81 cm) in the right lung and 0 – 2.8 cm (SD 0.83 cm) in the left lung. Among this cohort of 15 patients, 3 showed no diaphragmatic motion in the right hemidiaphragm secondary to a phrenic nerve palsy (see supplementary Movie 1). There was a corresponding compensation by the other lung with over 3 cm of diaphragmatic motion measured in each patient.

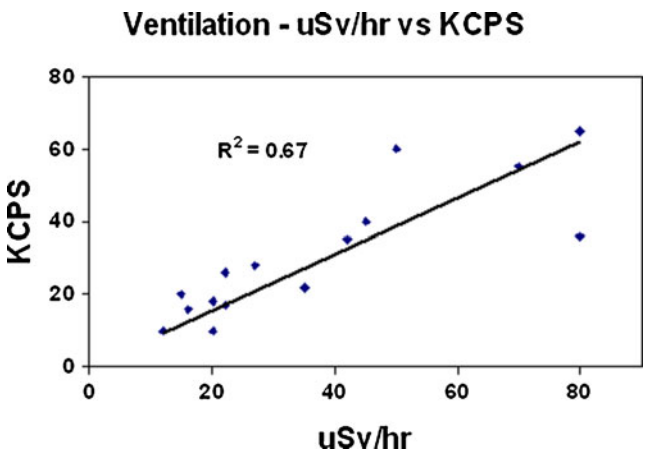

Fig. 1 Relationship between ventilation count rate on the Geiger counter and the count rate on the PET camera

Image coregistration

As shown in Table 1, the DC for both ventilation and perfusion scans were highest in group 3 (ExpPET/CT) and group 4 (FB-PET/AveCT) indicating the best volume overlap and therefore the best image coregistration between the modalities. The multiple comparison Tukey test's showed no significant difference in DC for either the ventilation or the perfusion scans between groups 3 and 4 ($p > 0.05$). There was a significant difference in DC for either the ventilation and the perfusion scans between groups 1 and 3, 1 and 4, 2 and 3, and 2 and 4 ($p < 0.05$). This indicates that group 1 (FB-PET/CT) and group 2 (InspPET/CT) had significantly poorer image coregistration than groups 3 and 4, as any differences between the groups could be attributed to misregistration between the PET and CT scans. Qualitative assessment of the image coregistration suggested that the poorer coregistration in groups 1 and 2 was primarily related to misregistration around the lung bases as shown in Fig. 2. This area is small in proportion to the overall lung volume, but the differences in image coregistration were consistent and significantly different. The PET and CT scans were best registered on the ExpPET/CT scans, which showed an absence of blurring around the lung bases. There was a substantial area of misregistration between the PET and CT scans around the lung based on both FB-PET/CT and InspPET/CT in most patients with preserved diaphragmatic motion.

Discussion

We found that ^{68}Ga-VQ 4-D PET/CT is feasible without additional scan time required compared to our previously described nongated technique [11]. In standard FB acquisition, the effects of respiratory motion on the images are unpredictable with resultant significant misregistration between the PET and CT scans. In this study we showed that adding respiratory gated scanning to a VQ-PET/CT scan enables any misregistration due to respiratory motion to be corrected. Our results showed that the benefit of adding 4-D scanning in terms of image co-registration is predominantly around the lung bases.

We also report evolving technical and practical considerations in performing VQ-PET/CT scanning. We showed that a simple hand-held Geiger counter is suitable for monitoring the amount of inhaled Galligas to obtain appropriate count rates on the subsequent PET acquisition. As in conventional VQ scanning, it is also possible to acquire sequential ventilation and perfusion scans by maintaining a suitable count rate ratio between the scans. As with Technegas, clumping of Galligas in the central airways can still result in shine-through of activity if an optimal VQ ratio is not achieved.

Table 1 Mean (SD) DC in the four groups

Group	Ventilation scans	Perfusion scans
1 (FB-PET/CT)	0.78 (0.09)	0.78 (0.08)
2 (InspPET/CT)	0.79 (0.07)	0.78 (0.08)
3 (ExpPET/CT)	0.82 (0.07)	0.80 (0.08)
4 (FB-PET/AveCT)	0.82 (0.07)	0.80 (0.08)

The long acquisition time of SPECT and PET introduces additional complexity in image interpretation as patients are breathing freely during scanning. As a result, activity in the lungs can be blurred due to continuous motion during the acquisition, particularly at the lung bases. This respiratory motion artefact can be corrected by using respiratory gating technology. This has been applied with conventional SPECT VQ scintigraphy, but is limited owing to inferior count statistics and lack of commercially available gating systems. A method to perform respiratory gating during a SPECT scan was described by Suga et al. who found improved lesion-to-normal lung contrast [13]. However, this technique only involves imaging the lungs in the end-inspiration position. An advantage of PET/CT is the availability of respiratory gating systems that permit 4-D acquisition of both PET and CT datasets [14, 15], allowing anatomical correlation of functional deficits. Additionally, respiratory gating of both PET and CT datasets enables accurate attenuation correction of the PET data to be performed for each bin.

There are multiple advantages of VQ PET/CT compared to conventional VQ scintigraphy. The addition of 4-D respiratory gating further enhances the PET technique with superior sensitivity, and spatial and temporal resolution compared to conventional scintigraphy [11]. In this study the blurring caused by respiratory motion on the FB-PET scan was well corrected on the 4-D PET scan. In particular, the expiration phase of the 4-D PET scan fused with the expiration 4-D CT scan showed excellent coregistration with no evident blurring. This could enable accurate monitoring of lung ventilation and perfusion over multiple time periods by having a relatively reproducible breathing position in the expiration phase as compared to the unpredictability of FB and deep inspiration lung positions. In institutions where a ^{68}Ge/^{68}Ga generator and a PET scanner are available the technique may be readily adopted as an alternative to conventional scintigraphy. The ability to more precisely quantify pulmonary blood flow and ventilation offers an opportunity to explore existing and new clinical applications in a variety of settings, particularly those where there is a clinical need to try to predict the consequences of radiation therapy or surgical lung interventions.

It is standard practice to use a 4-D AveCT scan for planning of radiotherapy [16]. In this cohort, we found that the 4-D AveCT reconstruction fused with a FB-PET scan provided

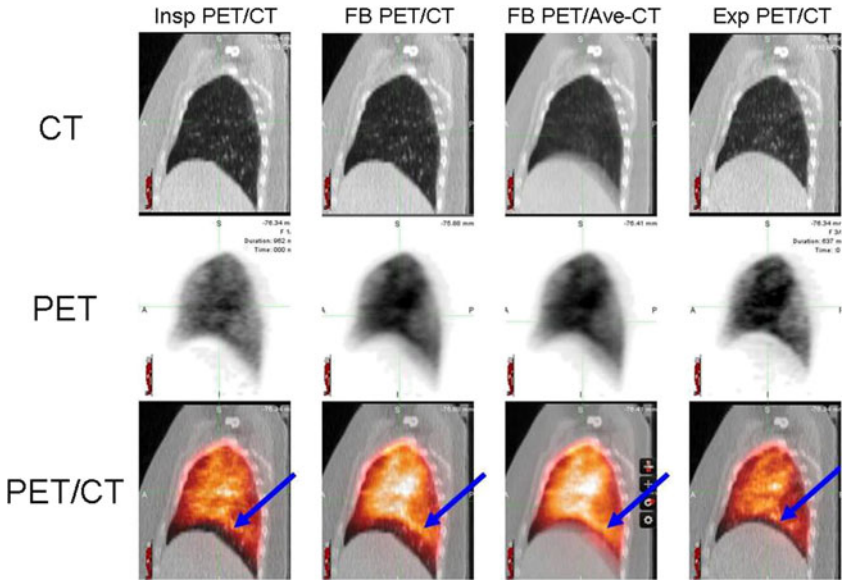

Fig. 2 Perfusion PET/CT showing effects of respiratory motion on image coregistration around the lung bases in the four groups analysed

much better coregistration than FB-PET/CT alone. In FB-CT the position of the diaphragm is random and therefore the amount of misregistration is unpredictable. Our results indicate that a FB-PET scan fused with an AveCT scan is the best combination for use in radiotherapy planning. The average imaging takes into account respiratory motion and removes the uncertainty caused by the random position of the diaphragm.

The 4-D CT data provides valuable additional information that may be clinically useful. In this series, we identified several patients with a phrenic nerve palsy and resultant compensatory increase in motion by the opposite lung. This has implications for planning of any target volumes in the compensating lung. In a recent study Dinkel et al. used 4-D MRI to analyse lung tumour motion in patients with a hemidiaphragmatic paralysis [17]. They found that the average displacement of the tumour was 6.6 mm as well a lateral shift of the mediastinum due to the compensatory effect of the unaffected lung. In these patients the increase in motion in the opposite lung has potential implications for dose deposition from radiation therapy in both the affected and compensating lungs. The addition of a 4-D CT scan, however, does potentially increase the radiation exposure for patients. However, to address this issue we lowered the 4-D CT exposure factors to a level that produces CTDI values similar to those of a noncontrast CT scan of the chest while still producing adequate image quality for this purpose.

Recently, studies have investigated using the information obtained from a 4-D CT scan to infer information about lung ventilation [18, 19]. However, as demonstrated in Fig. 3, aerated lung on CT images is not necessarily contributing to ventilation. Further, the 4-D CT ventilation techniques do not provide any information about lung perfusion, which is particularly relevant to radiation lung damage as the vascular endothelium is one of the most radiation-sensitive tissues in the lungs [20].

The limitations of this study include the lack of breathing training by the patients, leading to potentially poor coregistration between the inspiration phases of the CT and PET scans. A system such as the audiovisual biofeedback

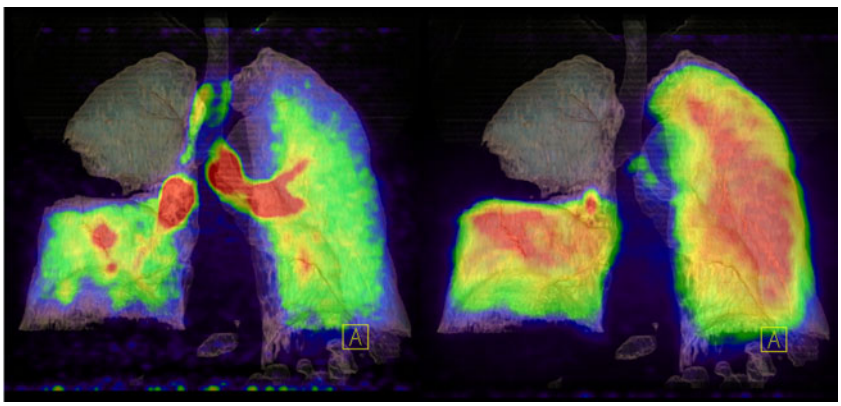

Fig. 3 Volume-rendered PET/CT images showing large areas of aerated lung in the right upper lobe with no evident ventilation (*left*) or perfusion (*right*). Precise coregistration of PET and CT datasets is provided with respiratory gated acquisition

method use for 4-D CT acquisitions as described by Cui et al. may improve coregistration between modalities in the inspiration phases [21]. However, this increases the complexity of acquisition as well as the time required on the scanner, potentially limiting its widespread use.

Conclusion

^{68}Ga-VQ 4-D PET/CT is feasible and the blurring caused by respiratory motion is well corrected with 4-D acquisition, which principally reduces artefact at the lung bases. The FB-PET/AveCT and ExpPET/CT scans produce images with the highest spatial overlap. The 4-D CT also provides valuable information. With its higher resolution compared to standard SPECT/CT, the ^{68}Ga-VQ 4-D PET/CT technique has a broad range of potential clinical applications including improving diagnostic algorithms for patients with suspected pulmonary embolism, preoperative evaluation of regional lung function and improving assessment or understanding of pulmonary physiology in the vast range of pulmonary diseases.

References

1. Wagner Jr HN, Sabiston Jr DC, Iio M, McAfee JG, Meyer JK, Langan JK. Regional pulmonary blood flow in man by radioisotope scanning. JAMA. 1964;187:601–3.
2. Leblanc M, Leveillee F, Turcotte E. Prospective evaluation of the negative predictive value of VQ SPECT using 99mTc-Technegas. Nucl Med Commun. 2007;28(8):667–72.
3. Jogi J, Jonson B, Ekberg M, Bajc M. Ventilation-perfusion SPECT with 99mTc-DTPA versus technegas: a head-to-head study in obstructive and nonobstructive disease. J Nucl Med. 2010;51(5):735–41.
4. Roach PJ, Gradinscak DJ, Schembri GP, Bailey EA, Willowson KP, Bailey DL. SPECT/CT in VQ scanning. Semin Nucl Med. 2010;40(6):455–66.
5. Hofman MS, Kong G, Neels OC, Eu P, Hong E, Hicks RJ. High management impact of Ga-68 DOTATATE (GaTate) PET/CT for imaging neuroendocrine and other somatostatin expressing tumours. J Med Imaging Radiat Oncol. 2012;56(1):40–7.
6. Buchmann I, Henze M, Engelbrecht S, Eisenhut M, Runz A, Schäfer M, et al. Comparison of 68Ga-DOTATOC PET and 111In-DTPAOC (Octreoscan) SPECT in patients with neuroendocrine tumours. Eur J Nucl Med Mol Imaging. 2007;34(10):1617–26.
7. Hicks RJ, Hofman MS. Is there still a role for SPECT-CT in oncology in the PET-CT era? Nat Rev Clin Oncol. 2012;9(12):712–20.
8. Kotzerke J, Andreeff M, Wunderlich G. PET aerosol lung scintigraphy using Galligas. Eur J Nucl Med Mol Imaging. 2010;37(1):175–7.
9. Mathias CJ, Green MA. A convenient route to [68Ga]Ga-MAA for use as a particulate PET perfusion tracer. Appl Radiat Isot. 2008;66(12):1910–2.
10. Kotzerke J, Andreeff M, Wunderlich G, Wiggermann P, Zophel K. Ventilation-perfusion-lungscintigraphy using PET and 68Ga-labeled radiopharmaceuticals. Nuklearmedizin. 2010;49(6):203–8.
11. Hofman MS, Beauregard JM, Barber TW, Neels OC, Eu P, Hicks RJ. 68Ga PET/CT ventilation-perfusion imaging for pulmonary embolism: a pilot study with comparison to conventional scintigraphy. J Nucl Med. 2011;52(10):1513–9.
12. Dice LR. Measures of the amount of ecologic association between species. Ecology. 1945;26(3):297–302.
13. Suga K, Yasuhiko K, Zaki M, Yamashita T, Seto A, Matsumoto T, et al. Assessment of regional lung functional impairment with co-registered respiratory-gated ventilation/perfusion SPET-CT images: initial experiences. Eur J Nucl Med Mol Imaging. 2004;31(2):240–9.
14. Nehmeh SA, Erdi YE, Pan T, Pevsner A, Rosenzweig KE, Yorke E, et al. Four-dimensional (4D) PET/CT imaging of the thorax. Med Phys. 2004;31(12):3179–86.
15. Callahan J, Kron T, Schneider-Kolsky M, Dunn L, Thompson M, Siva S, et al. Validation of a 4D-PET maximum intensity projection for delineation of an internal target volume. Int J Radiat Oncol Biol Phys. 2013;86(4):749–54.
16. Li G, Citrin D, Camphausen K, Mueller B, Burman C, Mychalczak B, et al. Advances in 4D medical imaging and 4D radiation therapy. Technol Cancer Res Treat. 2008;7(1):67–81.
17. Dinkel J, Hintze C, Tetzlaff R, Huber PE, Herfarth K, Debus J, et al. 4D-MRI analysis of lung tumor motion in patients with hemidiaphragmatic paralysis. Radiother Oncol. 2009;91(3):449–54.
18. Nyeng TB, Kallehauge JF, Hoyer M, Petersen JB, Poulsen PR, Muren LP. Clinical validation of a 4D-CT based method for lung ventilation measurement in phantoms and patients. Acta Oncol. 2011;50(6):897–907.
19. Yamamoto T, Kabus S, von Berg J, Lorenz C, Keall PJ. Impact of four-dimensional computed tomography pulmonary ventilation imaging-based functional avoidance for lung cancer radiotherapy. Int J Radiat Oncol Biol Phys. 2011;79(1):279–88.
20. Hill RP. Radiation effects on the respiratory system. BJR Suppl. 2005;27:75–81.
21. Cui G, Gopalan S, Yamamoto T, Berger J, Maxim PG, Keall PJ. Commissioning and quality assurance for a respiratory training system based on audiovisual biofeedback. J Appl Clin Med Phys. 2010;11(4):3262.